Published in final edited form as:
Nature. 2013 June 27; 498(7455): . doi:10.1038/nature12199.

Bach2 represses effector programmes to stabilize T_{reg}-mediated immune homeostasis

Rahul Roychoudhuri[1,*,±], **Kiyoshi Hirahara**[2,9,±], **Kambiz Mousavi**[3,±], **David Clever**[1], **Christopher A. Klebanoff**[1], **Michael Bonelli**[2], **Giuseppe Sciume**[2], **Hossein Zare**[3], **Golnaz Vahedi**[2], **Barbara Dema**[4], **Zhiya Yu**[1], **Hui Liu**[6], **Hayato Takahashi**[2], **Mahadev Rao**[1], **Pawel Muranski**[1], **Joseph G. Crompton**[1], **George Punkosdy**[5], **Davide Bedognetti**[6], **Ena Wang**[6], **Victoria Hoffmann**[7], **Juan Rivera**[4], **Francesco M. Marincola**[6,8], **Atsushi Nakamura**[10], **Vittorio Sartorelli**[3], **Yuka Kanno**[2], **Luca Gattinoni**[1], **Akihiko Muto**[10], **Kazuhiko Igarashi**[10], **John J. O'Shea**[2,*,†], and **Nicholas P. Restifo**[1,*,†]

[1]National Cancer Institute, National Institutes of Health (NIH), Bethesda, MD 20892, USA

[2]Molecular Immunology and Inflammation Branch, National Institute of Arthritis, Musculoskeletal and Skin Diseases (NIAMS), NIH, MD 20892, USA

[3]Laboratory of Muscle Stem Cells and Gene Regulation, NIAMS, NIH, MD 20892, USA

[4]Laboratory of Molecular Immunogenetics, NIAMS, NIH, MD 20892, USA

[5]National Institutes of Allergy and Infectious Diseases, NIH, Bethesda, MD, 20892, USA

[6]Department of Transfusion Medicine, NIH, Bethesda, MD 20892, USA

[7]Division of Veterinary Resources, NIH, Bethesda, MD 20892, USA

[8]Sidra Medical and Research Centre, Doha, Qatar

[10]Department of Biochemistry, Tohoku University, Sendai, Japan

Abstract

Through their functional diversification, distinct lineages of $CD4^+$ T cells play key roles in either driving or constraining immune-mediated pathology. Transcription factors are critical in the generation of cellular diversity, and negative regulators antagonistic to alternate fates often act in conjunction with positive regulators to stabilize lineage commitment[1]. Genetic polymorphisms within a single locus encoding the transcription factor BACH2 are associated with numerous autoimmune and allergic diseases including asthma[2], Crohn's disease[3–4], coeliac disease[5], vitiligo[6], multiple sclerosis[7] and type 1 diabetes[8]. While these associations point to a shared

[*]Correspondance and requests for materials should be addressed to R.R. (roychoudhuri@mail.nih.gov), J.O'S. (osheajo@mail.nih.gov) or N.P.R. (restifon@mail.nih.gov).
[9]Present address: Department of Advanced Allergology of the Airway, Graduate School of Medicine, Chiba University, Chiba, Japan.
[±]These authors contributed equally
[†]These authors contributed equally

Supplementary Information is linked to the online version of the paper at www.nature.com/nature.

Author contributions

R.R., K.H., J.O'S. and N.P.R. wrote the manuscript and designed experiments; R.R., K.H., K.M., D.C., M.B., G.S., Y.K., B.D., Z.Y., H.T. and H.L carried out experiments; R.R., H.Z., G.V., E.W., V.S., J.O'S and N.P.R. analyzed experiments; V.H. performed histopathological evaluations; G.P., A.N., A.M. and K.I contributed reagents; C.A.K., M.R., P.M., J.G.C., J.R., D.B., A.N., A.M., F.M., L.G., V.S. and K.I edited the manuscript.

 Massively parallel RNA and ChIP sequencing data have been deposited to the Gene Expression Omnibus under the accession number GSE45975.

The authors declare no competing financial interests.

mechanism underlying susceptibility to diverse immune-mediated diseases, a function for Bach2 in the maintenance of immune homeostasis has not been established. Here, we define Bach2 as a broad regulator of immune activation that stabilizes immunoregulatory capacity while repressing the differentiation programmes of multiple effector lineages in $CD4^+$ T cells. Bach2 was required for efficient formation of regulatory (T_{reg}) cells and consequently for suppression of lethal inflammation in a manner that was T_{reg} cell dependent. Assessment of the genome-wide function of Bach2, however, revealed that it represses genes associated with effector cell differentiation. Consequently, its absence during T_{reg} polarization resulted in inappropriate diversion to effector lineages. In addition, Bach2 constrained full effector differentiation within Th1, Th2 and Th17 cell lineages. These findings identify Bach2 as a key regulator of $CD4^+$ T-cell differentiation that prevents inflammatory disease by controlling the balance between tolerance and immunity.

Bach2 is expressed in B cells where it acts as a transcriptional repressor of Blimp-1 and is critical for somatic hypermutation and class switch recombination[9–11]. Given the association of polymorphisms in the *BACH2* locus with multiple inflammatory diseases in humans, we hypothesized an additional role for the transcription factor in the prevention of inflammation. To test this hypothesis, we characterized the phenotype of knockout (KO) mice in which the *Bach2* gene had been disrupted[9]. While pups appeared normal at birth, they developed a progressive wasting disease (Fig. 1a and Supplementary Fig. 1a) that resulted in diminished survival compared to wildtype (WT) littermates (Fig. 1b). Sera from KO mice at 3 months of age contained elevated levels of anti-nuclear and anti-dsDNA autoantibodies (Fig. 1c). Gross examination revealed enlargement of the lungs (Fig. 1d and Supplementary Fig. 1b) with highly penetrant histopathological changes (Fig. 1e) including extensive perivascular and alveolar infiltration by lymphocytes and macrophages (Fig. 1f). Examination of the gut revealed less severe and incompletely penetrant inflammatory pathology of the small intestine and stomach also associated with lymphocytic and macrophage infiltration (Fig. 1g and Supplementary Fig. 2). Consistently, we measured elevated expression of the C-C chemokine receptors CCR4 and CCR9 on splenic $CD4^+$ T cells, which guide migration to the lung and gut, respectively (Fig. 1h)[12–13]. Accordingly, we found a striking increase in the number of $CD4^+$ T cells in the lungs of KO animals while peripheral lymphoid organs contained similar or decreased numbers (Fig. 1i and Supplementary Fig. 3). We also observed increased proportions of effector cells in both the spleen and lungs of KO animals (Supplementary Fig. 4a) and a substantial proportion of $CD4^+$ T cells in lungs of KO animals expressed the acute activation marker CD69 (Fig. 1j and Supplementary Fig. 4b), a finding suggestive of their involvement in the inflammatory process affecting this organ. $CD4^+$ T cells can be characterized into a number of functionally specialized subsets depending upon expression of lineage-specific transcription factors and cytokines[14]. Th2 cells play a central role in allergic inflammation and airway disease and are characterized by expression of the transcription factor Gata3 and cytokines such as interleukin (IL)-4 and IL-13[15]. Consistent with the presence of Th2 inflammation, there were increased proportions of $Gata3^+$ $CD4^+$ T cells in the spleen and lungs (Fig. 1k and Supplementary Fig. 5) and elevated expression of IL-13 and IL-4 in the spleen, lungs and lymph nodes (LN) of KO animals (Fig. 1l and Supplementary Fig. 6a). By contrast, we observed no differences in the frequency of $IL\text{-}17A^+$ cells in these organs and only a minor increase in $IFN\text{-}\gamma^+$ cells in the LN (Supplementary Fig. 6b).

$CD4^+$ T cells play a key role in both driving and constraining immune-mediated pathology. While effector (T_{eff}) cells are often implicated in immune-mediated disease, $FoxP3^+$ T_{reg} cells suppress inflammatory reactions and play a non-redundant role in maintaining immune homeostasis[16–17]. Given dysregulated immune reactions in Bach2 KO animals, we measured expression of *Bach2* mRNA in conventional and regulatory $CD4^+$ T-cell subsets and their thymic precursors from *FoxP3*^{GFP} reporter mice. *Bach2* mRNA was expressed at

high levels in both conventional *FoxP3*$^-$ and *FoxP3*$^+$ (T_{reg}) CD4SP thymocytes in addition to naïve (T_{nai}) and T_{reg} cells in the spleen (Fig. 2a). Evaluation of conventional thymic maturation in KO animals revealed similar proportions of CD4SP, CD8SP and TCRβ$^+$ cells (Supplementary Fig. 7). Given high levels of expression of *Bach2* mRNA in CD4SP thymocytes, however, we wished to determine the cell-intrinsic function of Bach2 in regulating gene transcription within these cells. We therefore reconstituted *Rag1*$^{-/-}$ hosts with equal mixtures of lineage-depleted bone marrow cells (hereinafter, BM) from Ly5.1$^+$ WT and Ly5.1$^-$ KO animals and measured global gene expression in WT and KO CD4SP cells that had developed within the same host (Supplementary Fig. 8 and Supplementary Table 1). Gene set enrichment analysis (GSEA) of this dataset (Supplementary Table 2) indicated the loss of genes known to be dependent upon FoxP3[2] or directly bound by FoxP3 (Supplementary Fig. 9a)[18]. Consistent with these observations, mRNA encoding FoxP3 itself exhibited the greatest fold-reduction in expression amongst all transcripts measured (Fig. 2b and Supplementary Fig. 9b). Consequently, we observed a near complete absence of FoxP3$^+$ cells amongst KO CD4SP thymocytes in WT:KO mixed BM chimeric animals (Fig. 2c and Supplementary Fig. 10). In animals reconstituted with either KO BM alone (Fig. 2c) or equal mixtures of KO and FoxP3^{sf} BM (Supplementary Fig. 11), however, FoxP3$^+$ KO cells were present in both the thymus and spleen but at a lower frequency than amongst WT cells. Taken together, these findings indicated a cell-autonomous requirement for Bach2 in the formation of T_{reg} cells in the thymus with an incomplete defect in non-competitive environments.

While a proportion of T_{reg} cells found in peripheral tissues arise in the thymus (thymic T_{reg} or tT_{reg})[16], induced T_{reg} (iT_{reg}) cells develop from conventional FoxP3$^-$ CD4$^+$ T cells in extrathymic tissues. To test whether Bach2 was required for efficient formation of iT_{reg} cells, we tracked the fate of naïve CD4$^+$ T cells upon transfer into *Rag1*$^{-/-}$ hosts. While a proportion of WT CD4$^+$ T cells converted into FoxP3$^+$ iT_{reg} cells, significantly fewer KO cells underwent similar conversion (Supplementary Fig. 12). By contrast, KO cells exhibited similar stability of FoxP3 expression and survival upon transfer into *Rag1*$^{-/-}$ hosts over acute timepoints (Supplementary Fig. 13). Consistent with *in vivo* data, KO naïve CD4$^+$ T cells were markedly impaired in their ability to induce *FoxP3* mRNA and form FoxP3$^+$ iT_{reg} cells upon stimulation in the presence of TGF-β *in vitro* (Fig. 2d, Supplementary Fig. 14). Despite this, KO cells exhibited intact TGF-β and IL-2 signaling (Supplementary Fig. 15). Importantly, defective iT_{reg} induction in KO cells was rescued by reconstitution with *Bach2*-expressing retroviruses (Fig. 2e), confirming that Bach2 is required during induction for the formation of iT_{reg} cells. In addition, *Bach2* overexpression in WT cells enhanced FoxP3 induction under suboptimal polarizing conditions (Supplementary Fig. 16). Taken together, our results demonstrated a requirement for Bach2 in the efficient generation of both tT_{reg} and iT_{reg} cells. Accordingly, analysis of primary and secondary lymphatic tissues from KO mice at three months of age revealed a deficiency in T_{reg} cells resembling that in mice individually reconstituted with KO BM (Fig. 2f). Similar reduction in thymic T_{reg} cell frequency was observed in neonatal mice prior to evidence of autoimmune disease (Supplementary Fig. 17). Furthermore, T_{reg} cell formation was *Bach2* gene-dose dependent since mice heterozygous for the KO allele had reduced frequencies of T_{reg} cells (Supplementary Fig. 18). Thus, T_{reg} cells are found at low frequencies in KO mice despite the presence of inflammation in these animals. Characterization of these cells revealed higher levels of expression of T_{reg} cell suppressive molecules CD25, CTLA4 and GITR, the activation marker CD69 and the marker of terminal differentiation, KLRG1 (Fig. 2g and Supplementary Fig. 19; $P<0.05$)[19]. Consistent with this terminally differentiated phenotype, T_{reg} cells from Bach2-deficient mice failed to prevent colitis in long-term assays despite possessing acute suppressive function (Supplementary Fig. 20a–e)[19]. Since T_{reg} cells maintain immune homeostasis in an immunodominant fashion, disorders resulting from their deficiency are amenable to rescue by provision of wildtype T_{reg} cells. To test whether

failure to maintain immune homeostasis in the absence of Bach2 was a consequence of defective immunoregulatory capacity, we reconstituted lethally irradiated *Rag1*$^{-/-}$ mice with KO BM in the presence or absence of WT BM. Strikingly, while we observed massive induction of effector differentiation amongst KO CD4^{+} T cells and mucosal thickening of the large intestine accompanied by infiltration of KO cells, these changes were prevented by co-transfer of WT BM (Fig. 3a–b and Supplementary Fig. 21a). Consequently, animals reconstituted with KO BM exhibited profound weight-loss and diminished survival while co-transfer of WT BM prevented the induction of disease (Supplementary Fig 21b–c). The dominant immunoregulatory effect exerted by *Bach2* sufficient (WT) BM was dependent upon FoxP3 since BM from mice which possess an intact *Bach2* locus but lack functional FoxP3 protein (FoxP3^{Sf})[20] could not rescue the phenotype induced by KO BM (Fig. 3c). Moreover, the lethal phenotype induced by KO BM was rescued by transfer of purified splenic CD4^{+} CD25^{+} T_{reg} cells from WT mice. Thus, Bach2 is required for the prevention of lethal autoimmunity through its role in T_{reg} cell formation.

Taken together, these results demonstrated a non-redundant role for Bach2 in T_{reg}-mediated immune homeostasis. We wished, however, to determine the molecular mechanism by which it plays this role. For transcriptional repression, Bach2 is dependent upon a DNA-binding basic leucine zipper region located near the C-terminus of the protein[21]. We found that overexpression of a truncation mutant deficient in this region (Bach2$^{\Delta Zip}$) did not complement defective iT_{reg} induction in KO CD4^{+} T cells (Fig. 4a) implicating its function as a transcriptional regulator in T_{reg} cell formation. To identify genes whose expression is controlled by Bach2, we performed massively parallel RNA sequencing of KO naïve CD4^{+} T cells stimulated under iTreg polarizing conditions. Consistent with its role as a transcriptional repressor, a majority of differentially expressed genes were upregulated in Bach2-deficient cells (Supplementary Fig. 22). Strikingly, when we compared these genes with transcripts that were induced upon differentiation of naïve cells into effector-lineage Th1, Th2 or Th17 cells, we found that 31.8% (877) of all upregulated genes (2754) in Bach2-deficient cells were effector lineage-associated genes (Fig. 4b–c). To test whether Bach2 has a direct role in mediating these transcriptional differences, we measured genome-wide Bach2 binding in iT_{reg} cells by chromatin immunoprecipitiation with massively parallel sequencing (ChIP-Seq), validating selected loci by qPCR (Supplementary Fig. 23, Supplementary Table 7). Bach2 bound 43.6% of all derepressed genes including 408 derepressed effector-lineage associated genes (Fig. 4b–c). Examples from this group of genes are provided (Fig. 4d and Supplementary Fig. 24a); notably, Bach2 bound and repressed *Prdm1*, which encodes Blimp-1, a transcription factor critical in driving full effector differentiation in CD4^{+} T cells.[22] Bach2 also repressed genes with effector lineage-specific functions such as *Gata3*, *Irf4* and *Nfil3* and *Il12rb1*, *Il12rb2*, *Map3k8* and *Gadd45g* which play important roles in Th2 and Th1 differentiation respectively[23–27]. Additionally, Bach2 repressed *Ahr* which is involved in Th17 differentiation[28]. Importantly, a number of effector-lineage associated genes repressed by Bach2 encode proteins that transduce signals antagonistic to T_{reg} cell differentiation itself, including *Il12rb1, Il12rb2 and Tnfsf4*[29–30]. Repression of *Ccr4* and *Ccr9* by Bach2 (Supplementary Fig. 24b) was also of interest since it provides insight into the predominance of lung and gut immunopathology in KO animals.

These data indicated that an important aspect of the function of Bach2 is to repress the differentiation programmes of multiple effector lineages during iT_{reg} cell development. Consistently, KO CD4^{+} T cells stimulated under iT_{reg} conditions aberrantly expressed cytokines associated with effector lineages (Fig. 4e). To determine whether Bach2 stabilizes iT_{reg} cell development through repression of effector differentiation, we tested whether blockade of effector cytokines, which play an important role in positive-reinforcement of effector cell differentiation, could restore iT_{reg} induction in KO cells. While KO cells stimulated under iT_{reg} conditions preferentially differentiated into FoxP3^{-} cells expressing

T-bet, Gata3 or RORγt, master regulators of the Th1, Th2 and Th17 differentiation programmes, respectively (Fig. 4f), addition of neutralizing antibodies against IFN-γ and IL-4 partially reverted this phenotype, preventing aberrant induction of T-bet and Gata3 and restoring FoxP3 expression. Interestingly, Ror t expression in KO cells increased in the presence of α-IFN-γ and α-IL-4 antibodies, consistent with the recognized ability of IFN-γ and IL-4 to block Th17 differentiation. Consequently, higher levels of IL-17A were expressed by KO cells under these conditions (Supplementary Fig. 25). These observations raised the possibility that Bach2 might also constrain full effector differentiation amongst conventional T-cell subsets. Strikingly, and consistent with this hypothesis, we observed increased IFN-γ, IL-13 and IL-17A expression when KO naïve $CD4^+$ cells were stimulated under Th1, Th2 and Th17 conditions, respectively, indicating that additional to its role in T_{reg} cell development, Bach2 limits full effector differentiation in conventional $CD4^+$ T cells (Fig. 4g). During specification of a variety of tissues, negative regulators antagonistic to alternate fates often act in conjunction with positive regulators to stabilize lineage identity[1]. We have identified a function of Bach2 in repressing the differentiation programmes of multiple effector lineages in $CD4^+$ T cells. By doing so, Bach2 stabilizes the development of Treg cells while limiting full effector differentiation in conventional T cell lineages. Thus, at both a cellular and molecular level, Bach2 functions to constrain immune activation enabling it to play a critical role in the maintenance of immune homeostasis. These findings help explain the emergence of Bach2 as a key node in human autoimmunity.

Methods

Plasmid DNA and cloning

For the generation of pMSCV-IRES-Bach2-Thy1.1, a fragment of Bach2 cDNA was amplified by PCR from pMSCV-IRES-Bach2-EGFP[1] using the following primers: FW – 5′-GTATTAGCGG CCGCAGACCAT GGACTACAAGGACG ACGATGACAAG-3′ and RV – 5′-GATGAAATCG ATCTAGGCATA ATCTTTCC TGGGCTGT TCGTCCG-3′ and cloned into the NotI and ClaI sites within the multiple cloning site of pMSCV-IRES-Thy1.1-DEST (pMIT; Addgene 17442). pMIG-Bach2 and pMIG-Bach2$^{\Delta Zip}$ have been described previously[10].

Cell culture

$CD4^+$ T cells from spleens and lymph nodes of 6–8 week-old mice were purified by negative selection and magnetic separation (Miltenyi Biotec) followed by sorting of naïve $CD4^+CD62L^{high}CD44^-CD25^-$ cells using a FACSAria II sorter (BD). For isolation of T_{reg} cells, $CD4^+GFP^+$ cells were sorted from *FoxP3*^{GFP} reporter mice or $CD4^+CD25^{high}$ cells. Naïve $CD4^+$ T cells were activated by plate-bound anti-CD3 and soluble anti-CD28 (10 μg ml^{-1} each; eBioscience) in media for 3 days either under: Th0 conditions (media alone); Th1 conditions (IL-12 (20 ng ml^{-1}, R&D Systems) and anti-IL-4 neutralizing antibodies (10 μg ml^{-1}, BioXCell)); Th2 conditions (IL-4 (20 ng ml^{-1}, R&D Systems) and anti-IFN-γ neutralizing antibodies (10 μg ml^{-1}, BDPharmingen)); Th17 conditions (IL-6 (20 ng ml^{-1}, R&D Systems) plus human TGF-β1 (2 ng ml^{-1}, R&D Systems) and anti-IFN-γ neutralizing antibodies (10 μg ml^{-1}) and anti-IL-4 neutralizing antibodies (10 μg ml^{-1})) or iTreg conditions (IL-2 (100 IU ml^{-1}, R&D Systems) plus human TGF-β1 (5 ng ml^{-1})). Where indicated, purified naïve $CD4^+$ T cells were labeled with carboxyfluorescein succinimidyl ester (CFSE, 1mM, Molecular Probes) for 8 minutes at room temperature. The labeling reaction was quenched by washing in FCS.

Retroviral transduction

20ug of retroviral plasmid DNA along with 6ug pCL-Eco plasmid DNA were transfected using 60 ul Lipofectamine 2000 in 3 ml OptiMEM (Invitrogen) for 8 hours in antibiotic-free

media into Platinum-E ecotropic packaging cells (Cell Biolabs) plated a day prior on poly-D-lysine coated 10cm plates (Becton Dickinson) at a concentration of 6×10^6 cells per plate. Media were replaced 8 hours following transfection and cells were incubated for a further 48 hours. Retroviral supernatants were collected and spun at 2000 ×g for 2 hours at 32 °C onto 24 well non-tissue culture treated plates coated overnight in Retronectin (20 ug ml^{-1}; Takara Bio) and 5 ug ml^{-1} anti-CD3 (2C11) and 5 ug ml^{-1} anti-CD28 (37.51) (eBioscience). Supernatant was discarded and cells one day following stimulation were applied to plates in triplicate wells for 24 hours in the presence of polarizing cytokines.

Antibodies and flow cytometry

The following fluorescent dye-conjugated antibodies against surface and intracellular antigens were used: anti-FoxP3 (FJK-16s), anti-IL13 (eBio13A), anti-IL17A clone eBio17B7 and anti-Gata3 clone TWAJ (eBioscience); anti-Thy1.1 (OX-7), anti-Ly5.1 (A20), anti-KLRG1 (2F1), anti-B220 (RA3-6B2), anti-NK1.1 (PK136), anti-CTLA4 (UC10-4F10-11), anti-CD4 (RM4-5), anti-CD25 (PC61), anti-CD62L (MEL-14), anti-IFNg (Cat 554413), anti-IL4 (Cat 554435), anti-CD44 (IM7) and anti-CD8a clone 53-6.7 (BD Biosciences); anti-GITR Cat. FAB5241A (R&D Systems) and anti-CD19 clone 6D5 (Biolegend). Cells were incubated with specific antibodies for 30min on ice in the presence of 2.4G2 monoclonal antibody to block Fc R binding. All samples were acquired with a Canto II flow cytometer (Becton Dickinson) and analyzed using FlowJo software (TreeStar). Intranuclear staining for FoxP3 was carried out using the FoxP3 staining kit (eBioscience). To determine cytokine expression, cellular suspensions containing T cells were stimulated with phorbol 12-myristate 13-acetate, ionomycin and brefeldin-A (Leukocyte activation cocktail with Golgiplug; BD biosciences) for 4 h. After stimulation, cells were stained an amine- reactive exclusion-based viability dye (Invitrogen) and with antibodies against cell-surface antigens, fixed and permeabilized followed by intracellular staining with specific anti-cytokine antibodies. Single cell suspensions from lung tissues were prepared by mechanical disruption (GentleMACS, Miltenyi). Countbright beads were spiked-in for the flow cytometric quantification of absolute cell number (Invitrogen).

Autoantibody enzyme-linked immunosorbent assay (ELISA)

For measurement of antinuclear antibodies (ANAs) ELISA assays were performed on mouse serum according to the manufacturer's instructions (Alpha Diagnostic International). For the measurement of anti-dsDNA autoantiboties, dsDNA coated plates (Calbiotech, Inc.) were incubated with serum samples and anti-dsDNA titers were evaluated using a horseradish peroxidase-conjugated anti-mouse antibody (IgG, IgM, IgA) (Alpha Diagnostic International).

Quantitative reverse-transcription polymerase chain reaction (qRT-PCR)

Cells were sorted or transferred into RNALater solution (Ambion) and stored at −80 °C. Total RNA from pelleted cells was isolated using the RNAeasy mini kit (Qiagen). First-strand cDNA synthesis was performed using random priming using the high-capacity cDNA synthesis kit (Applied Biosystems) in the presence of SuperaseIn RNase inhibitor (Ambion). cDNA was used as a template for quantitative PCR reactions using the following Taqman primer-probes (Applied Biosystems): *Actb* (mm00607939_s1), *Bach2* (mm00464379_m1) and *Foxp3* (mm00475162_m1). Reactions were performed using Fast Universal PCR Mastermix (Applied Biosystems) according to manufacturer's instructions and thermocycled in quadruplicate 10uL reactions in 384-well plates using the Applied Biosystems. Signals in the FAM channel were normalized to ROX intensity, and *ct* values were calculated using automatically determined threshold values using SDS software (Applied Biosystems).

Bone marrow chimeras and Treg cell rescue experiments

For bone marrow reconstitution experiments, *Rag1*$^{-/-}$ mice were administered 1000Gy total-body γradiation from a ^{137}Cs source prior to intravenous injection of BM cells depleted of mature lineages from single-cell bone-marrow preparatons using antibody-coupled magnetic beads (Miltenyi). BM from 6–10 week old mice donor mice were used except from Scurfy mice where 12 day old pups were used as donors. Where indicated, 4 × 10^5FACS purified CD4$^+$ CD25$^+$ T cells were transferred intravenously into mice 1 day following transfer of BM cells.

In vivo iTreg induction

Rag1$^{-/-}$ mice were injected intravenously with 4 × 10^5 CD4$^+$CD25$^-$CD45RB^{high} cells from wild type or Bach2 deficient mice. On day 21 to 23, mononuclear cells were isolated from whole blood and analyzed for FoxP3 expression.

In vitro suppression assay

Varying numbers of WT and KO CD4$^+$CD25$^+$ T$_{reg}$ cells were cultured in 96-well round-bottom plates with 5 × 10^4 CFSE-labeled naïve CD4+CD62L$^+$CD44^{low} responder (T$_{resp}$) cells along with 1 ×10^4 MACS isolated CD11c$^+$ dendritic cells used as antigen-presenting cells (Miltenyi). Cells were stimulated with 1 μg ml^{-1} anti-CD3 antibody (BD Biosciences) for 72 h at 37°C and 5% CO_2. T$_{resp}$ cell proliferation was detected by flow cytometry.

In vivo suppression assay

In vivo suppression assays were done as previously described[31]. Briefly, *Rag2*$^{-/-}$ mice were injected intravenously with 1 × 10^5 CFSE-labeled naive CD4$^+$CD25$^-$CD45Rb^{hi} cells from CD45.1 mice with or without 1 × 10^5 wild type or Bach2-deficient CD4$^+$ *FoxP3*$^{GFP+}$ T$_{reg}$ cells. Mice were analysed on day seven for effector T-cell proliferation by flow cytometry.

Transfer colitis model

The transfer colitis model has been described previously[32]. Briefly, Rag1$^{-/-}$ mice were injected intravenously with 4 × 10^5 FACS-sorted naive CD4$^+$CD25$^-$CD45RB^{high} cells from CD45.1$^+$ mice with or without 1 × 10^5 WT or KO CD4$^+$CD25^{high} T$_{reg}$ cells. Mice were monitored weekly for weight loss and signs of disease, and killed at week 6. Sections of the proximal, mid-, and distal colon were fixed in buffered 10% formalin and stained with hematoxylin and eosin (H&E).

RNA Sequencing

RNA Sequencing was performed and analyzed as described previously[33]. Total RNA was prepared from approximately 1 million cells by using mirVana miRNA Isolation Kit (AM1560, ABI). 200 ng of total RNA was subsequently used to prepare RNA-seq library by using TruSeq SRRNA sample prep kit (FC-122-1001, Illumina) by following manufacturer's protocol. The libraries were sequenced for 50 cycles (single read) with HiSeq 2000 (Illumina). Sequence reads from each cDNA library were mapped onto the mouse genome build mm9 by using tophat, and the mappable data were then processed by Cufflinks (Trapnell BA Nat. Biotechnol 2010). The obtained data were normalized based on RPKM (reads per kilobase exon model per million mapped reads). To find differentially regulated genes, we used a 1.5-fold change difference between genotypes and 4-fold change difference between different lineages.

Chromatin Immunoprecipitation

T cells were chemically crosslinked and sonicated cells to generate fragmented genomic DNA. Chromatin immunoprecipitation was performed using an anti-Bach2 antibody (N-2; Tohoku University). For sequencing of immunoprecipitated DNA, DNA fragments were blunt-end ligated to the Illumina adaptors, amplified, and sequenced by using the Hi-Seq 2000 (Illumina, San Diego, CA). Sequence reads of 50 bps were obtained by using the Illumina Analysis Pipeline. All reads were mapped to the mouse genome (mm9), and only uniquely matching reads were retained. After removal of redundant reads, enriched peaks were called using ChIP-Seq analysis tool MACS[34]. Around 20000 peaks were detected at the *p*-value level of less than 10e-05 and FDR of less than 5%. Peaks in +/− 2kb vicinity of genes bodies were assigned to genes to identify the bound target genes. For PCR-based confirmation of Bach2 binding, chromatin immunoprecipitation was performed as described above, and qPCR reactions were carried out on input and immunoprecipitated DNA using the Power SYBR Green kit (Applied Biosystems) and primers as specified in Supplementary Table 7.

Microarray analysis

100 ng of total RNA extracted as previously described was amplified using Ovation® Pico WTA System V2 (NuGEN) according to the manufacturer's instructions. Briefly, first strand cDNA was synthesized using the SPIA tagged random and oligo dT primer mix in 10ul reaction after denaturation and incubated at 65 °C for 2 min and priming at 4 °C followed by extension at 25 °C for 30 min, 42 °C for 15 min and 77 °C for 15min. Second strand cDNA synthesis of fragmented RNA was performed using DNA polymerase at 4 °C for 1min, 25 °C for 10 min, 50 °C for 30 min and 80 °C for 20 min. 5′ SPIA tagged double stranded cDNA was used as the template for isothermal single strand cDNA amplification using the SPIA primer following a cycle of SPIA DNA/RNA primer binding, DNA replication, strand displacement and RNA cleavage at 4 °C for 1 min, 47 °C for 75 min and 95 °C for 5min in total 100 ul reaction. 5.5 ug of amplified sscDNA from 12–13 ug total amplification were used for fragmentation and biotinilation using Encore™ Biotin Module (NuGEN) according to the manufacturer's instructions. Biotinylated cDNA was then hybridized to Mouse Gene 1.0 ST arrays (Affymetrix) overnight at 45 °C and stained on a Genechip Fluidics Station 450 (Affymetrix), all according to the respective manufacturers' instructions. Arrays were scanned on a GeneChip Scanner 3000 7G (Affymetrix). Global gene expression profiles rank ordered by relative fold-change values were analyzed by using Gene set enrichment analysis software (Broad Institute, MIT). *P* values were calculated using Student's *t*-test using Partek Genomic Suite after RMA normalization.

Statistical analysis

Student's *t*-test was used unless otherwise specified to calculate statistical significance of the difference in mean values and P values are provided. For calculation of statistical significance of differences in clinical histopathology scores, the Wilcoxon rank-sum test was used.

Supplementary Material

Refer to Web version on PubMed Central for supplementary material.

Acknowledgments

This research was supported by the Intramural Research Programs of the US National Institutes of Health, National Cancer Institute, National Institute of Arthritis, Musculoskeletal and Skin Diseases and the JSPS Research Fellowship for Japanese Biomedical and Behavioural Researchers at NIH (K.H.). We thank D.N. Roychoudhuri,

D.C. Macallan, G.E. Griffin, Y. Ji, D. Palmer, M. Sukumar, G. Fabozzi, K Hanada, E. Lugli, J.H. Pan and N.Van Panhuys for discussions, A. Mixon and S. Farid for cell sorting, G. McMullen for mouse handling and Y. Luo, Y. Wakabayashi, J. Zhu, G. Gutierrez-Cruz and H.W. Sun for help with sequencing and analysis.

References

1. Rothenberg EV, Scripture-Adams DD. Competition and collaboration: GATA-3, PU.1, and Notch signaling in early T-cell fate determination. Semin Immunol. 2008; 20:236–246. [PubMed: 18768329]
2. Ferreira MA, et al. Identification of IL6R and chromosome 11q13.5 as risk loci for asthma. Lancet. 2011; 378:1006–1014. [PubMed: 21907864]
3. Franke A, et al. Genome-wide meta-analysis increases to 71 the number of confirmed Crohn's disease susceptibility loci. Nat Genet. 2010; 42:1118–1125. [PubMed: 21102463]
4. Christodoulou K, et al. Next generation exome sequencing of paediatric inflammatory bowel disease patients identifies rare and novel variants in candidate genes. Gut. 2012
5. Dubois PC, et al. Multiple common variants for celiac disease influencing immune gene expression. Nat Genet. 2010; 42:295–302. [PubMed: 20190752]
6. Jin Y, et al. Genome-wide association analyses identify 13 new susceptibility loci for generalized vitiligo. Nat Genet. 2012; 44:676–680. [PubMed: 22561518]
7. International Multiple Sclerosis Genetics C et al. Genetic risk and a primary role for cell-mediated immune mechanisms in multiple sclerosis. Nature. 2011; 476:214–219. [PubMed: 21833088]
8. Cooper JD, et al. Meta-analysis of genome-wide association study data identifies additional type 1 diabetes risk loci. Nat Genet. 2008; 40:1399–1401. [PubMed: 18978792]
9. Muto A, et al. The transcriptional programme of antibody class switching involves the repressor Bach2. Nature. 2004; 429:566–571. [PubMed: 15152264]
10. Ochiai K, et al. Plasmacytic transcription factor Blimp-1 is repressed by Bach2 in B cells. J Biol Chem. 2006; 281:38226–38234. [PubMed: 17046816]
11. Muto A, et al. Bach2 represses plasma cell gene regulatory network in B cells to promote antibody class switch. EMBO J. 2010; 29:4048–4061. [PubMed: 20953163]
12. Sigmundsdottir H, Butcher EC. Environmental cues, dendritic cells and the programming of tissue-selective lymphocyte trafficking. Nat Immunol. 2008; 9:981–987. [PubMed: 18711435]
13. Lloyd CM, et al. CC chemokine receptor (CCR)3/eotaxin is followed by CCR4/monocyte-derived chemokine in mediating pulmonary T helper lymphocyte type 2 recruitment after serial antigen challenge in vivo. J Exp Med. 2000; 191:265–274. [PubMed: 10637271]
14. O'Shea JJ, Paul WE. Mechanisms underlying lineage commitment and plasticity of helper CD4+ T cells. Science. 2010; 327:1098–1102. [PubMed: 20185720]
15. Zhu J, Yamane H, Paul WE. Differentiation of effector CD4 T cell populations (*). Annu Rev Immunol. 2010; 28:445–489. [PubMed: 20192806]
16. Sakaguchi S, Fukuma K, Kuribayashi K, Masuda T. Organ-specific autoimmune diseases induced in mice by elimination of T cell subset. I. Evidence for the active participation of T cells in natural self-tolerance; deficit of a T cell subset as a possible cause of autoimmune disease. J Exp Med. 1985; 161:72–87. [PubMed: 3871469]
17. Gavin MA, et al. Foxp3-dependent programme of regulatory T-cell differentiation. Nature. 2007; 445:771–775. [PubMed: 17220874]
18. Zheng Y, et al. Genome-wide analysis of Foxp3 target genes in developing and mature regulatory T cells. Nature. 2007; 445:936–940. [PubMed: 17237761]
19. Cheng G, et al. IL-2 receptor signaling is essential for the development of Klrg1+ terminally differentiated T regulatory cells. J Immunol. 2012; 189:1780–1791. [PubMed: 22786769]
20. Brunkow ME, et al. Disruption of a new forkhead/winged-helix protein, scurfin, results in the fatal lymphoproliferative disorder of the scurfy mouse. Nat Genet. 2001; 27:68–73. [PubMed: 11138001]
21. Oyake T, et al. Bach proteins belong to a novel family of BTB-basic leucine zipper transcription factors that interact with MafK and regulate transcription through the NF-E2 site. Mol Cell Biol. 1996; 16:6083–6095. [PubMed: 8887638]

22. Crotty S, Johnston RJ, Schoenberger SP. Effectors and memories: Bcl-6 and Blimp-1 in T and B lymphocyte differentiation. Nat Immunol. 2010; 11:114–120. [PubMed: 20084069]
23. Rengarajan J, et al. Interferon regulatory factor 4 (IRF4) interacts with NFATc2 to modulate interleukin 4 gene expression. J Exp Med. 2002; 195:1003–1012. [PubMed: 11956291]
24. Zheng W, Flavell RA. The transcription factor GATA-3 is necessary and sufficient for Th2 cytokine gene expression in CD4 T cells. Cell. 1997; 89:587–596. [PubMed: 9160750]
25. Murphy KM, et al. Signaling and transcription in T helper development. Annu Rev Immunol. 2000; 18:451–494. [PubMed: 10837066]
26. Watford WT, et al. Tpl2 kinase regulates T cell interferon-gamma production and host resistance to Toxoplasma gondii. J Exp Med. 2008; 205:2803–2812. [PubMed: 19001140]
27. Kashiwada M, Cassel SL, Colgan JD, Rothman PB. NFIL3/E4BP4 controls type 2 T helper cell cytokine expression. EMBO J. 2011; 30:2071–2082. [PubMed: 21499227]
28. Veldhoen M, et al. The aryl hydrocarbon receptor links TH17-cell-mediated autoimmunity to environmental toxins. Nature. 2008; 453:106–109. [PubMed: 18362914]
29. Xiao X, et al. OX40 signaling favors the induction of T(H)9 cells and airway inflammation. Nat Immunol. 2012; 13:981–990. [PubMed: 22842344]
30. Oldenhove G, et al. Decrease of Foxp3+ Treg cell number and acquisition of effector cell phenotype during lethal infection. Immunity. 2009; 31:772–786. [PubMed: 19896394]
31. Pesu M, et al. T-cell-expressed proprotein convertase furin is essential for maintenance of peripheral immune tolerance. Nature. 2008; 455:246–250. [PubMed: 18701887]
32. Powrie F, Carlino J, Leach MW, Mauze S, Coffman RL. A critical role for transforming growth factor-beta but not interleukin 4 in the suppression of T helper type 1-mediated colitis by CD45RB(low) CD4+ T cells. J Exp Med. 1996; 183:2669–2674. [PubMed: 8676088]
33. Vahedi G, et al. STATs shape the active enhancer landscape of T cell populations. Cell. 2012; 151:981–993. [PubMed: 23178119]
34. Zhang Y, et al. Model-based analysis of ChIP-Seq (MACS). Genome Biol. 2008; 9:R137. [PubMed: 18798982]

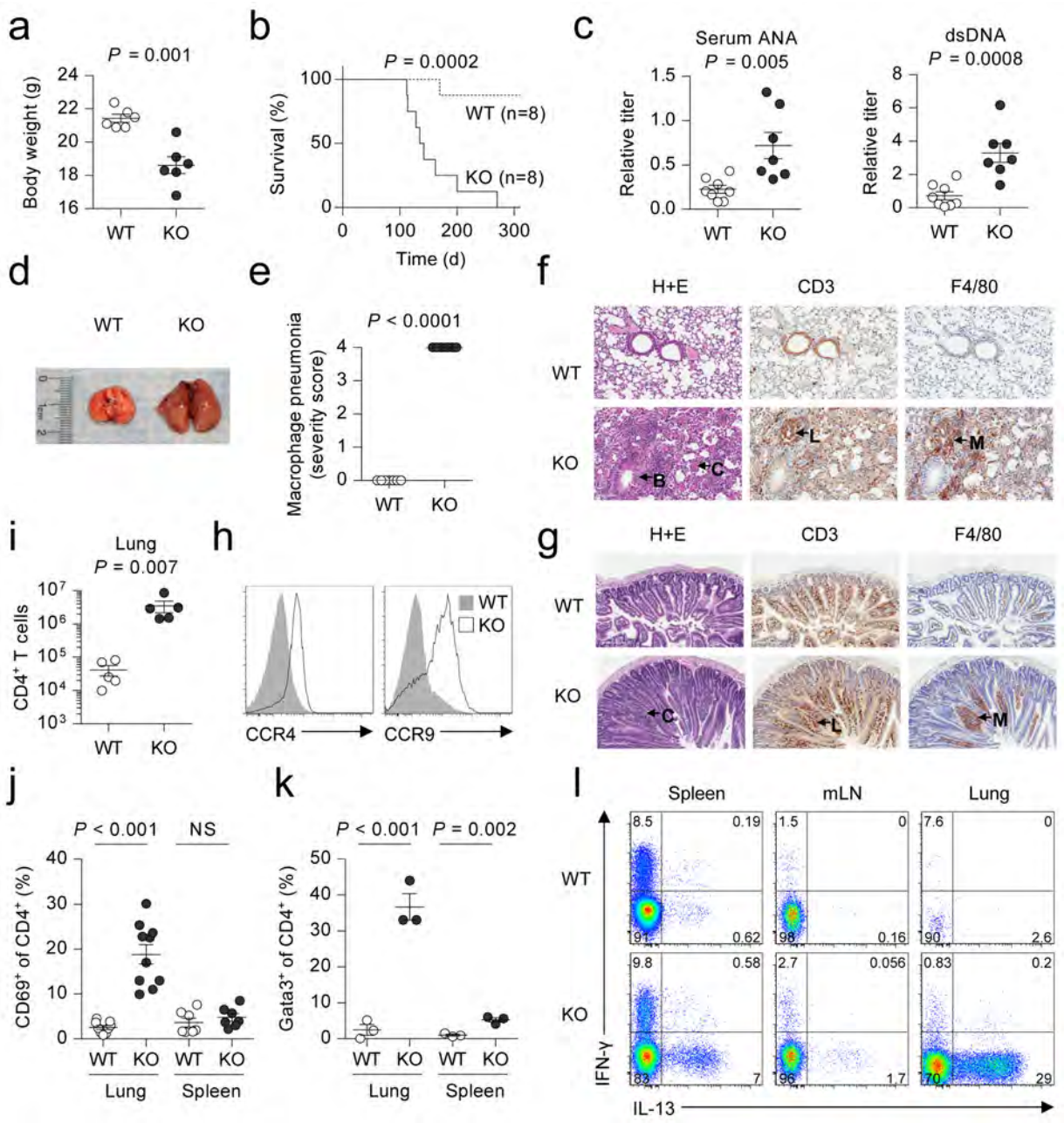

Figure 1. Spontaneous lethal inflammation in Bach2 knockout animals

a,b, Body weight at three months of age (**a)** and survival (**b)** of Bach2 knockout (KO) and wildtype (WT) littermate females. **c,** Titer of anti-dsDNA antibodies and anti-nuclear antibodies (ANA) in the sera of WT and KO animals. **d,** Gross morphology of lungs from WT and KO mice. **e,** Histopathology scoring of lung tissue from WT and KO mice (n = 7 per group). **f,** Haematoxylin and eosin (H+E) and immunohistochemical (IHC) stains of WT and KO lung tissue with hypertrophy of bronchial epithelium (B), eosinophilic crystals (C), perivascular lymphocytic infiltration (L) and macrophage infiltration (M). **g,** H+E and IHC stains of small intestinal tissue with hypertrophic crypts (C), lymphocytic infiltration (L) and macrophage infiltration (M). **h,** Expression of CCR4 and CCR9 on the surface of splenic $CD4^+$ T cells. **i,** Quantification of $CD4^+$ T cells in lungs of WT and KO animals. **j, k,**

Percentage of $CD4^+$ T cells expressing CD69 (**j**) and Gata3 (**k**) in the lungs and spleen. **l,** Flow cytometry of IFN-γ and IL-13 expression by $CD4^+$ T cells from spleen, mLN and lungs. Mice were analyzed at 3 months of age unless otherwise specified. Data are representative of ≥2 independent experiments with ≥3 mice per genotype. Error bars s.e.m.; *P* values (Student's *t*-test).

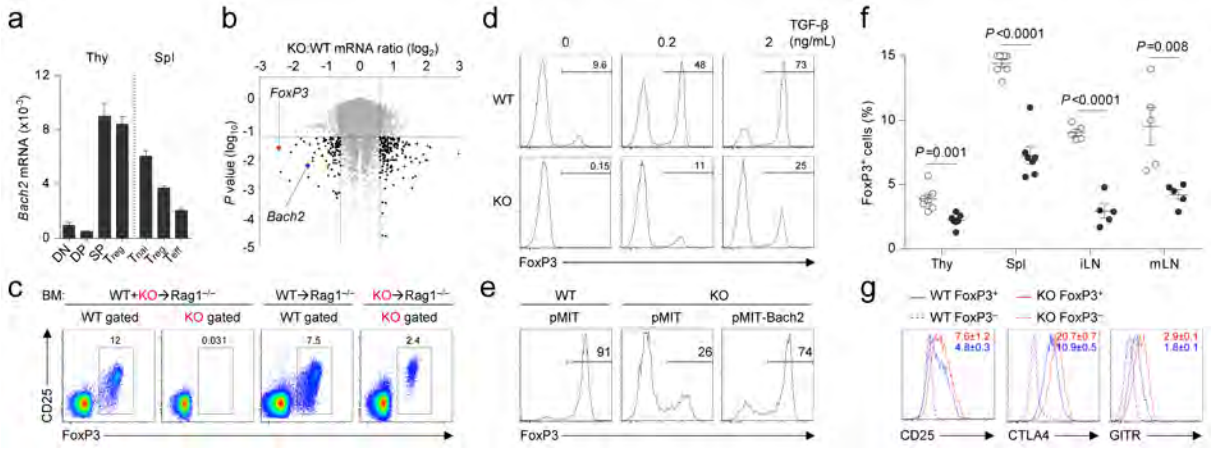

Figure 2. Bach2 is required for efficient formation of Treg cells

a, Expression of *Bach2* mRNA in thymic *FoxP3*$^{GFP-}$ DP and CD4SP (SP), and *FoxP3*$^{GFP+}$ CD4SP Treg cells and splenic CD4^{+} *FoxP3*$^{GFP-}$ Tnai and Teff, and *FoxP3*$^{GFP+}$ Treg cells isolated from *FoxP3*^{GFP} reporter mice relative to *Actb* mRNA. **b,** Volcano plot indicating differentially expressed genes in KO compared with WT CD4SP thymocytes from WT:KO mixed BM chimeric animals. **c,** Intracellular FoxP3 expression in CD4SP thymocytes from mice reconstituted with individual or mixed transfers of WT and KO BM. **d,** FoxP3 expression in WT and KO naïve splenic CD4^{+} T cells stimulated in the presence of indicated amounts of TGF-β *in vitro*. **e,** FoxP3 expression in Thy1.1^{+} (transduced) WT and KO naïve splenic CD4^{+} T cells stimulated in the presence of 2ng ml^{-1} TGF-β and transduced with indicated retroviruses. **f,** Ratio of FoxP3^{+} cells in thymic (gated on CD4SP) and extrathymic tissues (gated on CD3^{+}CD4^{+}cells) of 3 month old WT and KO littermates. **g,** Expression of CD25, CTLA4 and GITR on the surface of splenic FoxP3^{+} and FoxP3^{-} CD4^{+} cells from WT and KO mice. Error bars s.e.m.; *P* values (Student's *t*-test). All data are representative ≥2 independent experiments with ≥3 mice per genotype (**a–c, f–g)** or ≥ 4 experiments (**d–e)**.

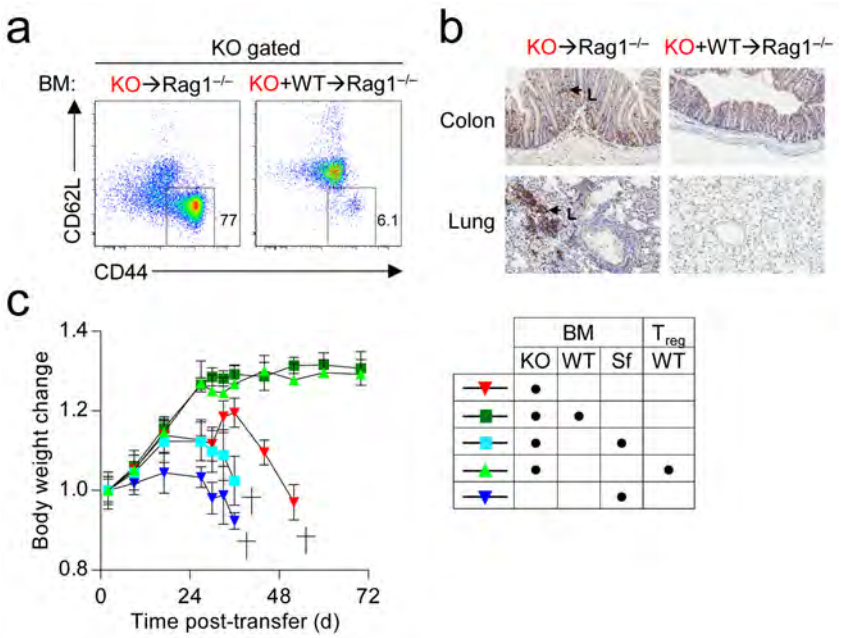

Figure 3. Bach2 is required for suppression of lethal inflammation in a Treg-dependent manner

a, CD44 and CD62L expression on splenic $CD4^+$ T cells descended from KO BM 6 weeks following individual or mixed reconstitution of *Rag1*$^{-/-}$ mice with KO and WT BM. **b,** CD3 staining of large intestine and lung tissue from mice 6 weeks following reconstitution with indicated BM. Arrows indicate KO T cells (L). **c,** Mass of mice following individual or mixed reconstitution of *Rag1*$^{-/-}$ mice with BM from Scurfy (FoxP3^{sf}), KO or WT mice with or without transfer of 4×10^5 purified splenic $CD4^+$ $CD25^+$ Treg cells. Data are representative of ≥3 independent experiments. Mass measurements were continued until <3 mice were remaining (**c**). Error bars s.e.m.; *P* values (Student's *t*-test).

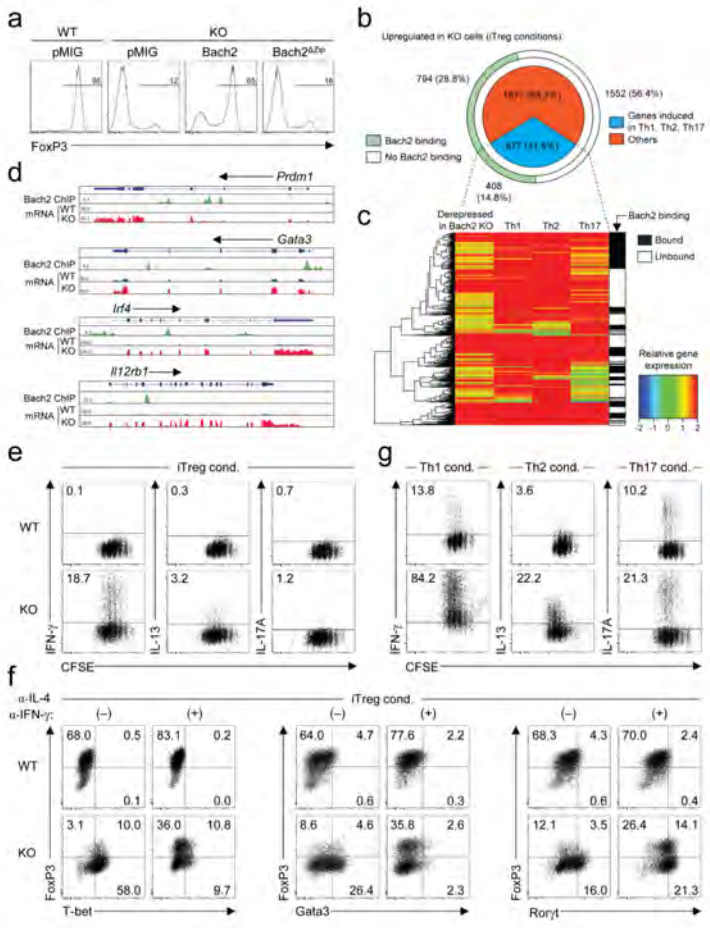

Figure 4. Bach2 represses effector programmes to stabilize iTreg cell development

a, FoxP3 expression in GFP$^+$ (transduced) WT and KO naïve splenic CD4$^+$ T cells stimulated in the presence of 2ng ml^{-1} TGF-β and transduced with indicated retroviruses. **b,** Derepressed genes in KO compared with WT naïve CD4$^+$ T cells stimulated under iTreg polarizing conditions. Proportion of effector-lineage associated transcripts (upregulated upon stimulation of naïve CD4+ T cells in Th1, Th2 or Th17 conditions respectively (pie chart) and genes that are directly bound by Bach2 in iTreg cells (outer arc) are shown. **c,** Heatmap indicating expression of effector-lineage associated transcripts derepressed in KO cells (iTreg conditions), their expression in wildtype Th1, Th2 and Th17 cells and binding at their respective gene loci by Bach2 (gene-body ±2kb). **d,** Alignments showing binding of Bach2 to selected genes and their mRNA expression in WT and KO cells cultured under iTreg conditions. **e,** Proliferation and effector cytokine expression in CFSE-labelled WT and KO naïve CD4$^+$ T cells stimulated under iTreg conditions for 3 days. **f,** Transcription factor expression upon stimulation of WT and KO naïve CD4$^+$ T cells under iTreg conditions for 3 days in the presence or absence of indicated anti-cytokine neutralizing antibodies. **g**, Proliferation and effector cytokine expression in CFSE-labelled WT and KO naïve CD4$^+$ T cells stimulated under indicated polarizing conditions for 3 days. Data are representative of ≥2 independently repeated experiments (**a,e–g).**